Journal Name

ARTICLE

Combined *in-* and *ex-situ* studies of pyrazine adsorption into the aliphatic MOF Al-CAU-13: structures, dynamics and correlations

Received 00th January 20xx,
Accepted 00th January 20xx

DOI: 10.1039/x0xx00000x

www.rsc.org/

Helge Reinsch,[a*] Jannik Benecke,[a] Martin Etter,[b] Niclas Heidenreich[a,b] and Norbert Stock[a*]

The intercalation of different pyrazines (pyrazine, methylpyrazine, 2,5-dimethylpyrazine, 2,3-dimethylpyrazine, trimethylpyrazine and tetramethylpyrazine) into the *trans*-1,4-cyclohexanedicarboxylate (CDC^{2-}) based Al-MOF [Al(OH)(CDC)], denoted as CAU-13, was investigated. The adsorption of the guest molecules into the flexible MOF was carried out from aqueous solution or via vapour phase adsorption, starting with the hydrated narrow-pore form of the framework $[Al(OH)(O_2C\text{-}C_6H_{10}\text{-}CO_2)]\cdot H_2O$ (CAU-13-*np*). The obtained host-guest systems were characterised by thermogravimetry and vibrational spectroscopy and their crystal structures were elucidated using powder X-ray diffraction (PXRD) data. The crystal structures indicate that guest molecules forming hydrogen-bonds with the host framework (pyrazine, methylpyrazine and 2,5-dimethylpyrazine) induce a slight opening of the channels, resulting in a semi-open framework conformation (CAU-13-*so*). For the bulkier guests 2,3-dimethylpyrazine, trimethylpyrazine and tetramethylpyrazine, only Van der Waals contacts can be observed between the host and the guest molecules and the large pore conformation is observed (CAU-13-*lp*). We carried out *in-situ* PXRD studies using synchrotron radiation during the adsorption of the respective guest molecules from aqueous solutions with various concentrations and at different temperatures. In general, stronger host-guest interactions required milder adsorption conditions while harsher conditions nevertheless accelerated the conversion. The kinetic parameters for the intercalation of pyrazine indicate that the rate limiting step differs, depending on the intercalation temperature.

Introduction

During the recent two decades there has been a steadily growing interest in the group of compounds denoted as metal-organic frameworks (MOFs). Such materials are most often formed by the connection of cationic inorganic building units (e.g. isolated ions or metal-oxo-clusters or chains) via anionic or neutral organic building units (e.g. amines, carboxylates or azolates).[1] This allows in theory the replacement of building units by topologically equivalent ones, yielding compounds with tailored properties. MOFs exhibiting permanent porosity were shown to be suitable candidates for this approach named isoreticular synthesis.[2] Thus the porosity and surface properties can be easily tuned to yield materials with remarkable performance in fields of application like adsorption,[3] catalysis,[4] luminescence[5] or energy storage.[6] Furthermore, MOFs sometimes show remarkable properties which are rarely paralleled by other crystalline materials. One outstanding phenomenon is the tremendous flexibility of some frameworks, which is induced by an external stimulus like temperature, pressure or by the presence of guest molecules.[7] In case this behaviour is fully reversible, it is denoted as "breathing".[8] The most intensely investigated breathing MOFs are the MIL-88-[9] and the MIL-53-series[10] (MIL stands for Material Institute Lavoisier). The latter framework with composition [M(OH)BDC] (BDC^{2-} = 1,4-benzenedicarboxylate) is known to form from a variety of inorganic cations like Sc^{3+},[11] Cr^{3+},[12] Fe^{3+},[13] Al^{3+},[14] Ga^{3+} [15] and In^{3+}.[16] The joint inside the framework which allows for its flexibility is the axis connecting the oxygen atoms of the carboxylate groups. Rotation around this axis yields the closed pore or the open pore form of the 1D-channels in the framework. This particular mechanism is known as "knee-cap" mechanism.

In more recent years, several related frameworks were reported which, in some cases, also show breathing behaviour. Replacement of the aromatic terephthalate anions by its aliphatic counterpart *trans*-1,4-cyclohexanedicarboxylate (CDC^{2-}) results in frameworks with MIL-53-topology and composition [M(III)(OH)CDC], which could be first obtained using In^{3+} or Cr^{3+}.[17,18] Employing this linker molecule in combination with Al^{3+} or Ga^{3+} yields also frameworks with MIL-53-topology[19] which were moreover reported to exhibit the breathing phenomenon.[20,21] However, in these compounds denoted CAU-13 (CAU stands for Christian-Albrechts-

[e] Institute of Inorganic Chemistry
Christian-Albrechts-University Kiel
Max-Eyth-Straße 2
24118 Kiel, Germany
Email: stock@ac.uni-kiel.de
[b] Deutsches Elektronen Synchrotron (DESY)
Notkestr. 85
22607 Hamburg, Germany

Electronic Supplementary Information (ESI) available: Details of the Rietveld refinements, crystallographic information files, vibrational spectra, TG curves and additional information on the *in-situ* experiments. See DOI: 10.1039/x0xx00000x

University) the changes in framework structure are mostly due to rotations around the torsionally flexible C-C bonds in the linker molecule, while the influence of the "knee-cap" is only of minor importance. This eventually can also induce a change in the conformation of the linker molecules inside the framework (Fig. 1). While different conformers are observed in the narrow pore form (*a,a*- and *e,e*-orientation of the carboxylate groups), only the *e,e*-conformer is observed in the large pore form of the CAU-13 framework.

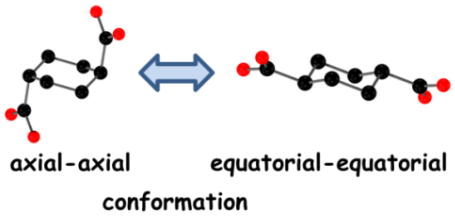

Figure 1: Representation of the conformational flexibility of the *trans*-cyclohexanedicarboxylate linker (CDC^{2-}) as it is observed for example in CAU-13 MOFs.

A similar behaviour was also reported for the Ti^{4+}-based MOF $[Ti_3(\mu_3\text{-}O)O_2(CDC)_3]$ or COK-69 (COK stand for Centrum voor Oppervlaktechemie en Katalyse).[22] This MOF exhibits a topology identical to MIL-88, but while the latter shows breathing which is induced by the knee-cap mechanism, the different forms of COK-69 contain either a mixture of *a,a*- and *e,e*-conformers of *trans*-1,4-cyclohexanedicarboxylate (open pore form) or solely the *a,a*-conformer (closed pore form). Similarly the zirconium based MOF $[Zr_6O_4(OH)_4(CDC)_6]$ exhibits two different framework conformations.[23] The large pore form containing polar solvents is highly crystalline with cubic symmetry and solely the *e,e*-conformation of CDC^{2-} is observed. The narrow pore form obtained upon solvent removal is only weakly crystalline and tetragonally distorted, which is induced by a partial change in conformation of the linker molecules. Thus the *e,e*- and the *a,a*-conformers are present in 1:2 ratio. An even less rigid linker molecule has been employed to obtain a MIL-53-type structure based on the aliphatic single chain linker adipic acid (hexanedioic acid).[24] In this compound the breathing motion between a dry and a hydrated framework is also dominated by conformational changes of the aliphatic chain. This also leads to substantial disorder in the open framework conformation, apparently since the various conformations of adipate ions are easily interconvertible.

The aforementioned observations indicate that the breathing behaviour in aliphatic MIL-53 frameworks can substantially differ from the effects observed in the aromatic compounds. Thus, here we present a study on the intercalation of pyrazines with differing degree of methylation into Al-CAU-13 (Figure 2). The products were characterised regarding structure and composition to elucidate the dominant interactions between host and guests.

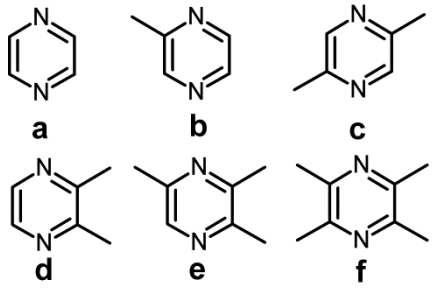

Figure 2: The guest molecules employed for intercalation into Al-CAU-13. From left to right, top row: pyrazine (**a**), methylpyrazine (**b**), 2,5-dimethylpyrazine (**c**). Bottom row: 2,3-dimethylpyrazine (**d**), trimethylpyrazine (**e**), tetramethylpyrazine (**f**).

Powder X-ray diffraction studies during crystallisation or phase transitions are an ideal tool to shed light on the kinetics of such processes. Using high intensity synchrotron radiation also allows for the measurement of diffraction data for solids forming inside a closed reaction vessel.[25] Thus the crystallisation of, for example, simple oxides like TiO_2[26] or doped CeO_2[27] as well as more complex oxometallates[28], thioantimonates[29], thiostannates[30], gallophosphates[31] and other materials[32,33,34] was already investigated. In addition the crystallisation of MOFs has recently also come into focus.[35,36,37,38,39] Improvement of the experimental set-up enabled just very recently the in-situ observation of the exchange of coordinated solvent molecules in a Yb-based MOF[40] and this technique was also employed to study the breathing behaviour of Fe-MIL-53 during adsorption of aromatic guests from aqueous solutions.[48]

In-situ powder X-ray diffraction experiments measured during the adsorption process for the different pyrazine derivatives from aqueous solution into Al-CAU-13 gave further insight into the product formation.

Experimental

Materials. All used chemicals are commercially available and were employed without further purification.

Methods. The synthesis of Al-CAU-13 was carried out in Pyrex glass bottles with screw cap and a volume of 100 mL based on the published procedure.[21] Powder X-ray diffraction (PXRD) data were collected on a STOE Stadi P diffractometer equipped with a Mythen detector using monochromated $CuK\alpha_1$ radiation in transmission geometry. All processing of the crystallographic data was done with TOPAS.[41] IR-spectra were measured on a Bruker ALPHA-FT-IR A220/D-01 spectrometer equipped with an ATR-unit. The thermogravimetric analyses were recorded using a NETZSCH STA 429 CD analyzer with a heating rate of 4 K min^{-1} under flowing air (flow rate 75 ml min^{-1}). The force field based geometry optimizations were carried out using the forcite package available in the Materials Studio software based on the implemented Universal Force Field (UFF).[42]

Synthesis. Al-CAU-13 (**1**) was synthesised from a mixture of 1.448 g (6 mmol) $AlCl_3 \cdot 6H_2O$, 1.022 g (6 mmol) H_2CDC, 8 mL H_2O and 32 mL dimethylformamide (DMF) in a 100 mL Pyrex

bottle. The reactor was sealed and placed in an oven which was heated up to 130 °C over 1 h, kept at this temperature for 12 h and cooled down to ambient conditions over 1 h. The raw product was filtered off, washed with additional DMF and acetone and dried overnight at 120 °C in air.

For the intercalation of the different pyrazines, several methods were investigated and the approach yielding the compound with highest crystallinity was chosen for full characterisation. Thus pyrazine, 2,3-dimethylpyrazine, trimethylpyrazine and tetramethylpyrazine were adsorbed via the gas phase. For this purpose, 15 mg of the hydrated Al-CAU-13 were placed inside a small Teflon jar and this small jar was placed in a larger Teflon reactor which was filled with 100 mg (pyrazine or tetramethylpyrazine) or 200 µL (2,3-dimethylpyrazine or trimethylpyrazine) of the respective guest. The container was put into a steel autoclave and placed in a preheated oven (120 °C) for 3 h.

The other pyrazines were intercalated from aqueous solutions. Thus 50 mg of **1** and 1.5 mL of a 2 M solution of 2,5-dimethylpyrazine were stirred for 1 h at ambient conditions and filtrated. Similarly, methylpyrazine was intercalated by heating 1.5 mL of a 5 M solution containing 50 mg **1** to 40 °C under stirring for 1 h.

Results and Discussion

Structures and Properties

The crystal structures were determined using PXRD data. Details on the procedures and the final Rietveld plots can be found in the supporting information. In general, a suitable model of the host framework was developed by indexing of the patterns and finding a suitable, already reported parent structure, which was optimised by force-field optimisation. Subsequently, the respective guest molecules were generated and considered as rigid bodies. Eventually the structure models obtained in this manner were confirmed by Rietveld refinement. Please note that hydrogen bonding between aromatic nitrogen atoms and oxygen atoms of the framework was evaluated by measuring the interatomic distances since protons cannot be localised by means of Rietveld refinement using powder X-ray diffraction data.

The resulting structures can be divided into two categories, dominated either by the presence of hydrogen bonding or by Van der Waals interactions. First the compounds dominated by hydrogen bonds will be discussed. Some relevant parameters of the refinements are shown in Table S1 (see SI).

The linker molecules are in general present in *a,a*- and *e,e*-conformation in 1:1 molar ratio, showing a very similar framework conformation as in Ga-CAU-13 containing DMF molecules.[20] Compared to the hydrated Al-CAU-13, this subtle opening is only induced by slight rotations around C-C bonds in the aliphatic linker molecules while the *a,a*-conformation of the linker is retained.[19]

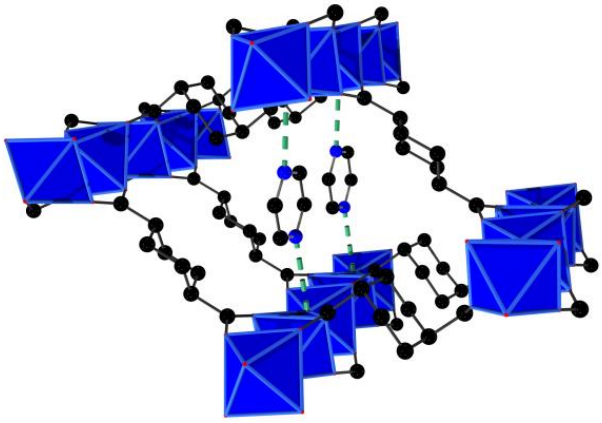

Figure 3: The crystal structure of pyrazine loaded CAU-13 **1a** seen along the *a*-axis. AlO_6 polyhedra in blue, carbon atoms in black and nitrogen atoms in blue. Dashed green lines indicate hydrogen bonds.

In **1a**, the pyrazine molecules are assembled around the inversion centre and bound to the µ-OH groups (which are interconnecting the aluminium ions) in a pincer-like fashion (Fig. 3). Two different O···N distances are observed which indicate moderate interactions between the OH-groups and the guests (N···O distances of 3.05(1) and 3.12(1) Å).[43]

The host-guest compound containing methylpyrazine, **1b**, exhibits a different bonding motif. Apparently the methyl group prevents its adjacent basic nitrogen atom from hydrogen bonding and therefore only the "free" basic sites are interacting with the µ-OH groups of the inorganic building units (Fig. 4). While this results in only half the number of binding sites compared to **1a**, the bonding in **1b** is considerably stronger (N···O distance of 2.79(1) Å).

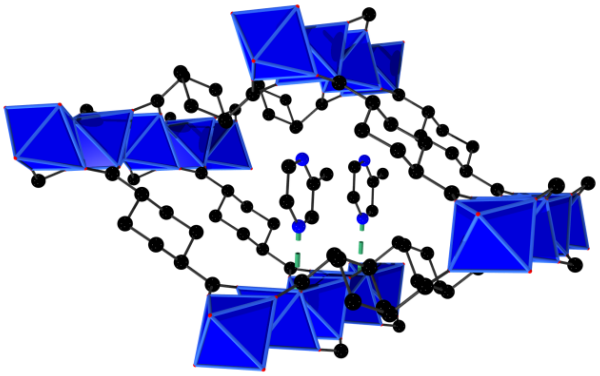

Figure 4: The crystal structure of methylpyrazine loaded CAU-13 **1b** seen along the *a*-axis. AlO_6 polyhedra in blue, carbon atoms in black and nitrogen atoms in blue. Dashed green lines indicate the observed hydrogen bonds.

The structure of the MOF containing 2,5-dimethylpyrazine guest molecules, **1c**, shows strong similarities to the one of compound **1b**. The guest molecules are bound only via one nitrogen atom to the µ-OH groups with an intermediate N···O-distance (3.00(2) Å). The second N···O-distance indicates only very weak (if any) hydrogen bonding (3.50(2) Å). However, due to the higher number of methyl groups and their steric demand, a smaller number of guest molecules per formula

unit could be localised upon increase of the molecule size (for **1a**: 0.484(2) pyrazine molecules per Al^{3+}; for **1b**: 0.397(3) methylpyrazine molecules per Al^{3+}; for **1c**: 0.22(1) 2,5-dimethylpyrazine molecules per Al^{3+}). Additional electron density observed inside the channels of **1c** was refined as oxygen atoms. However, we assume that additional guest molecules are adsorbed in a non-ordered fashion.

The other investigated guest molecules adsorb without the formation of hydrogen bonds. Nevertheless, there are substantial differences observed in the crystal structures. Some relevant parameters are summarized in Tab. S2.

Only compound **1d** containing 2,3-dimethylpyrazine exhibits a crystal structure in which the guest molecules are unambiguously arranged in an ordered fashion (Fig. 5). The distances between the adsorbed 2,3-dimethylpyrazine molecules (> 4 Å) do not indicate any strong interaction between the guests and thus we assume that the ordered adsorption and the resulting symmetry result from a packing effect. This is also substantiated by the slightly lower cell volume for **1d** compared to **1e** and **1f** and the higher loading with guest molecules.

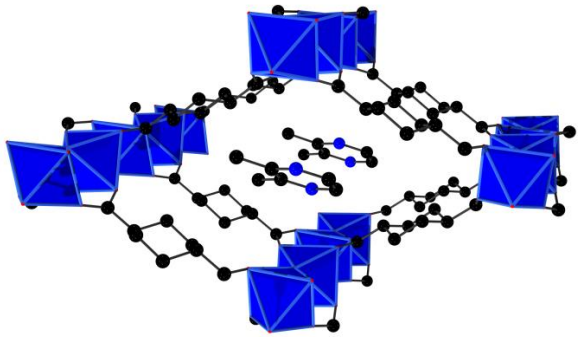

Figure 5: The crystal structure of 2,3-dimethylpyrazine loaded CAU-13 **1d**. AlO_6 polyhedra in blue, carbon atoms in black and nitrogen atoms in blue.

The compounds **1e** and **1f** both exhibit a very similar framework conformation as **1d** but their symmetry is higher (orthorhombic *I*-centred instead of monoclinic *C*-centred). The guest molecules also assemble in the centre of the channels. However, we rather assume that these structures represent a case of non-ordered arrangement of guest molecules, which is only "modelled" by the refined structures. This would be in line with the observed higher space group symmetry, which is the highest observed yet for [M(III)(OH)(CDC)] structures. Other structures with weakly binding guests like **1d** and Al-CAU-13 loaded with xylene[21] all exhibit lower symmetry. The distances between framework and guest molecules in **1d**, **1e** and **1f** indicate no strong interactions and thus the structures are dominated by weak Van der Waals forces. Nevertheless the amount of intercalated guest molecules differs for each of these guests (for **1d**: 0.500(5) 2,3-dimethylpyrazine molecules per Al^{3+}; for **1e**: 0.420(6) trimethylpyrazine molecules per Al^{3+}; for **1f**: 0.418(8) tetramethylpyrazine molecules per Al^{3+}), possibly due to the steric demand of the larger molecules.

The differing binding modes of the guest molecules are also clearly visible in the IR-spectra of the compounds (Fig. 6, for more detailed spectra see SI). The IR-spectra indicate that the guest molecules bearing more CH_3-groups lead to stronger absorption in the spectral range for C-H stretching vibrations (especially at 2922 cm^{-1}). Moreover the presence and absence of hydrogen bonds between host and guest can be also clearly deduced from the spectra. The structures which are dominated by Van der Waals interactions (compounds **1d**, **1e** and **1f**) show a sharp peak at ≈ 3690 cm^{-1} for the free O-H stretching vibration of the μ-OH group in the inorganic building unit. In the other spectra (for **1a**, **1b** and **1c**) this peak is substantially broadened and therefore much less pronounced. This can be clearly attributed to the formation of hydrogen bonds between host and guest in these compounds.

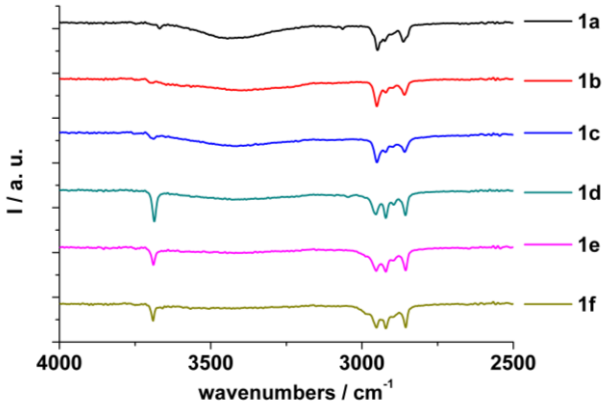

Figure 6: IR-spectra of the described compounds in the range 4000 – 2500 cm^{-1}. The complete spectra can be found in the SI.

In order to validate the observed occupancies of the guest molecules after Rietveld refinement we also carried out thermogravimetric (TG) measurements (see SI). By relating the observed weight losses to each other we deduced the amount of adsorbed guest molecules. In all curves a small weight loss is observed below 100 °C, which we attribute to the desorption of water molecules adsorbed on the particle surface. The other observed values for the weight losses between 100 and 300 °C and above 300 °C are tabulated in Tab. 1. In all samples the weight loss above 300 °C, which corresponds to the combustion of the framework, is lower than expected. We attribute this to the presence of X-ray amorphous impurities like aluminium oxides or hydroxides which are often observed in the synthesis of Al-MOFs, but mostly visible in thermogravimetric experiments.[44,45] The ratio of guest : MOF was therefore deduced from the ratio of weight losses above 100 °C (attributed to the desorption of the respective pyrazine) and above 300 °C (attributed to the combustion of one CDC^{2-} linker anion).

The deduced molar host : guest ratios are mostly in reasonable agreement with the values observed during Rietveld refinement. Only for the compound **1c** incorporating 2,5-dimethylpyrazine, a strong discrepancy is found. As mentioned above, additional electron density was observed during

Rietveld refinement, which could be due to the co-adsorption of water molecules or due to the adsorption of additional guest molecules in a non-ordered fashion. This could also explain the higher weight loss observed in the TG curve compared to the amount of guests observed in the refined crystal structure.

Table 1: The observed fractional weight losses and residues for the respective host-guest compounds and the expected weight losses and deduced molar ratios as they were observed in the thermogravimetric experiments.

Compound	**1a**	**1b**	**1c**	**1d**	**1e**	**1f**
Δm_1 (100–300°C) [%]	16	11.8	13.8	19.4	17.7	20
Δm_2 (> 300°C) [%]	61.5	61.9	62.1	57.9	58.1	57.7
residue [%]	22.5	23.8	24.1	22.7	24.2	22.3
expected Δm_2 [%]	71	76	77	72	77	71
guest: linker ratio	0.53	0.33	0.33	0.50	0.40	0.41
Rietveld ratio	0.48	0.39	0.22	0.50	0.42	0.41

The results presented up to now can be directly compared to the host-guest structures of MOFs with MIL-53 framework (thus aromatic counterparts of CAU-13 with formula [M(III)(OH)(BDC)]) formed by heteroaromatic compounds. A MOF with Fe-MIL-53 structure exhibits a rather open framework conformation for the compound intercalated with pyridine.[46] The guest molecules are strongly bound to the μ-OH groups with an N-O distance of 2.68(2) Å. For Al-MIL-53 two different structures were reported with adsorbed pyridine, which depend on the amount of loaded guest molecules.[47] Both exhibit a fully open framework conformation and both show similar hydrogen bonding as Fe-MIL-53. The very same effect can be also observed for Ga-MIL-53 upon pyridine adsorption.[47] The adsorption of lutidine (2,6-dimethylpyridine) in Fe-MIL-53 was also investigated.[48] In this case the guest is initially only bound via a mediating water molecule between the lutidine and the μ-OH groups to result in an open framework. Upon careful desorption of water, a host-guest complex with directly hydrogen bonding guest molecules can be obtained, in which the framework is slightly compressed. The described bonding in Al-CAU-13 is substantially different since two distinct framework forms are observed which differ in the ratio of linker conformers (*e,e* vs. *a,a*). Moreover the fully open framework conformation is only observed when no hydrogen bonds are present and the amount of loaded guest molecules is much lower compared to MIL-53. We propose that this could be a result of the kinked shape of the CDC^{2-} molecules and the higher number of protons bound to the aliphatic ring. These differences might suffice to slightly shield the μ-OH groups from the bulkier guest molecules. The substantial structural differences of the title compounds inspired us also to investigate the adsorption process for Al-CAU-13 by means of *in-situ* powder X-ray diffraction using synchrotron radiation.

In-situ PXRD studies

Herein we used the system Al-CAU-13 / guest /H_2O as a model system for *in-situ* PXRD studies. This was enabled by the construction of a new reactor cell which will be described elsewhere in more detail.[49] The core of the reaction cell is a pressure resistant Pyrex glass tube which is inserted into a temperature controlled heating mantle (Fig. 7).

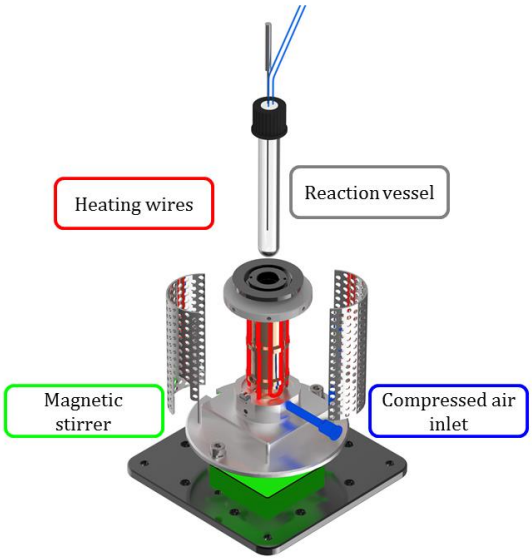

Figure 7: Schematic presentation of the in-situ reactor used in this study.

A temperature sensor inside the tube allows the regulation by controlling heating (mantle) and cooling power (pressurised air). A magnetic stirrer agitates the reaction mixture inside the tube, which is also equipped with connections to up to two syringe pumps. This allows for the addition of reactants after preheating the reaction mixture and therefore also permits a precisely defined starting point of a reaction.[50] In this study Al-CAU-13 (**1**) was preheated in water to a preset temperature and once this temperature was reached, the respective guest molecules were added as an aqueous solution or in pure liquid form.

Prior to the investigations at the synchrotron radiation source, the conditions under which the hydrated MOF **1** is fully converted to the respective host-guest complex were established by ex-situ experiments. Thus depending on the guest molecule, different reaction conditions were chosen in order to achieve complete conversion, which is a prerequisite for the kinetic analysis.[51] Tetramethylpyrazine was not further investigated in these experiments since it is not sufficiently soluble in H_2O. The optimised reaction conditions are summarised in Tab. 4. In all experiments, 50 mg **1** and 1.5 mL H_2O were first transferred into the reaction cell and after reaching the designated temperatures the respective pyrazine solution was added to the mixture by a syringe pump under vigorous stirring.

Table 2: The reaction conditions investigated by in-situ PXRD experiments.

Guest	product	Added V [mL]	solution	T [°C] minimum
pyrazine	**1a**	1.5	4M	40
methylpyrazine	**1b**	1.5	pure	40
2,5-dimethylpyrazine	**1c**	1.5	4M	40
2,3-dimethylpyrazine	**1d**	1.5	pure	70
trimethylpyrazine	**1e**	1.5	pure	90

PXRD data were recorded throughout these experiments using monochromated radiation (60 keV, 0.207 Å) with collecting times of 30 seconds per pattern at beamline P02.1 at Petra III, DESY, Hamburg. The resulting time resolved PXRD data for the adsorption of pyrazine at 40 °C are exemplarily shown in Fig. 8. Further data are shown in the supporting information (Fig. S19 –Fig. S23, Fig. S28). The large halo around 3.5 ° can be attributed to diffuse scattering due to the reactor materials and the solvent inside the reactor. For the evaluation of the data, we focussed on the low angle range below 2 °. In this range the diffraction signals of hydrated **1** are clearly visible at the beginning of the reaction. Upon addition of the aqueous pyrazine solution after 8 minutes, an increase in background scattering can be observed. Moreover, the MOF begins immediately to convert to the host-guest compound **1a**. However, this reaction proceeds very rapidly (within ≈16 minutes at 40°C) and at higher temperatures the conversion is accelerated.

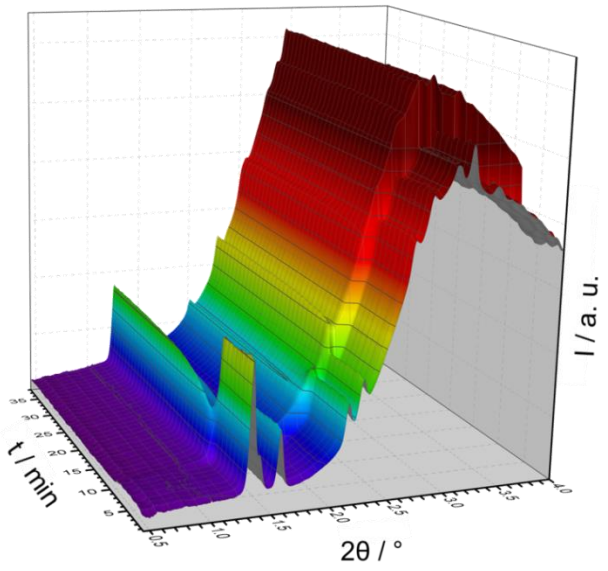

Figure 8: 3D plot for the conversion of **1** to **1a** at 40 °C (wavelength 0.207 Å).

For most guest molecules, the pure reagent was added to the MOF dispersion which also results in very fast adsorption. The higher temperatures required for full conversion to **1d** or **1e** did also lead to a virtually instantaneous conversion to the respective guest loaded forms. The reactions were considered complete once the intensity of the product peaks did not increase further and the reaction times are summarised in Tab. 3, depending on the respective guest and temperature. For the intercalation of trimethylpyrazine to yield **1e**, no reliable data can be given since the high viscosity of the reaction mixture led to the formation an inhomogeneous slurry which resulted in strong fluctuations of the measured diffraction intensities. Moreover small peaks of the starting compound **1** remained visible in the measured patterns However, the reaction seems to be similarly fast as for the adsorption of 2,3-dimethylpyrazine to form **1d**.

Table 3: Conversion times for the reaction of **1** to the respective host guest complex depending on temperature. For the compounds **1b**, **1d** and **1e**, the pure liquid was added while for **1a** and **1c** a 4 M aqueous solution was used.

Compound	**1a**	**1b**	**1c**	**1d**	**1e**
T = 40 °C	16 min	4 min	7 min		
T = 50 °C	6 min	1 min	2 min		
T = 60 °C	3 min	1 min	1 min		
T = 70 °C	1 min	1 min	1 min	2 min	
T = 80 °C				1 min	
T = 90 °C				1min	incomplete

From the first inspection of these values, it is obvious that the guest molecules which are only interacting via weak Van der Waals forces with the host require higher intercalation temperatures and higher guest concentrations for the complete conversion. The reason for the higher required temperature could be a larger activation energy for the transition from the narrow pore form to the large pore form. The intercalations leading to **1a, 1b** and **1c** result in the semi-open pore framework and thus no conformational change of the guest molecules is necessary. The conformational change of the linker molecules from *a,a*- to *e,e*-conformation for **1d** and **1e** results in an increased kinetic barrier. Moreover, this inhibition could be also affected by entropy. One must keep in mind that approximately 1 guest molecule of 2,3-dimethylpyrazine or trimethylpyrazine replaces ≈ 2.5 water molecules which are interacting by hydrogen bonding in **1**.

The slowest intercalation reactions are observed for the adsorption of pyrazine and 2,5-dimethylpyrazine at 40 °C starting from diluted aqueous solutions. Methylpyrazine, while also interacting via hydrogen bonds, does require the addition of the pure guest compound for full conversion and thus also adsorbs comparably fast. In general, adsorption of the guest molecules interacting via hydrogen bonds is achieved at much milder conditions and thus seems to be more favoured (also taking into account that H_2O acting as competing guest molecule is still present in excess). Guest molecules forming only weaker Van der Waals interactions require harsher reaction conditions for adsorption, which is most likely due to a higher kinetic barrier resulting from the conformational transition of the linker molecules.

The short reaction times make a kinetic analysis of the breathing phase transition upon adsorption challenging and, to the best of our knowledge, no such investigation has been reported yet. Since the duration of the intercalation reaction is comparably long for the formation of **1a**, data with higher temporal resolution was measured at a beamline with higher photon flux (P08 at PETRA III, DESY, Hamburg) allowing for a

temporal resolution of 10 s per pattern. The formation of the intercalated compound **1a**, which also corresponds to the reaction progress α, was evaluated at different temperatures. The peak maximum of the 010 reflection was considered proportional to the amount of product formed. Conventionally, this proportionality is deduced from the peak area, but due to peak overlap and the limited resolution of the detector, integration of the peaks was unsuccessful. The observed curves are shown in Figure 9.

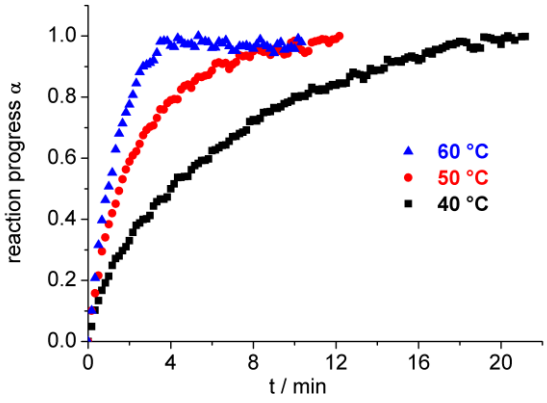

Figure 9: Reaction progress α depending on the respective temperature for the conversion of **1** to **1a**.

Higher temperatures clearly accelerate the conversion to form **1a** and thus the conversion is completed after ≈ 20, 11 and 3 minutes at 40, 50 and 60°C, respectively. This data can be moreover analysed using the Sharp-Hancock plot.[51] Plotting ln(-ln(1-α)) against ln(t) should result in an approximately linear correlation with the slope m and the intercept m*ln(k), at least in case the reaction mechanism is unchanged during the course of the reaction. The evaluated constant m is called the Avrami exponent and its value is usually characteristic for the reaction mechanism, ideally indicating a slowest and thus rate limiting reaction step. Moreover, the apparent reaction rate constant k can be also deduced. Using this method, we observed linear correlations up to values for α > 0.9. The corresponding plots can be found in the supporting information (Fig. S24-S26) and the observed kinetic parameters are summarized in Tab. 4. These values numerically confirm that the reaction is clearly accelerated at higher temperatures.

Table 4: Kinetic parameters for the adsorption of pyrazine into Al-CAU-13 as determined by Sharp-Hancock analysis.

temperature	Linear till	m	k [min^{-1}]
40 °C	α = 0.94	0.90(1)	0.166
50 °C	α = 0.99	0.95(1)	0.366
60 °C	α = 0.96	1.24(2)	0.637

The values of the Avrami exponent are in a range which is typical for reactions limited by diffusion (m = 0.4-0.7) or phase-boundary controlled (m ≈ 1.1). However, the Avrami model actually is a nucleation/crystal growth model which is not necessarily applicable for the breathing of MOFs or similar reactions. In addition this model is based on the classical theory that initially nuclei are formed which subsequently grow into larger crystallites.[52] While this is not necessarily the case for the breathing of Al-CAU-13, it is a potential scenario. However, this means that these values are unlikely to have any true physical meaning in the context of a breathing MOF.

An Arrhenius plot of ln(k) against 1/T yields the slope E_{Act}/R and thus gives an estimation of the activation energy for the adsorption of pyrazine (see SI). The value amounts to 58(5) kJ/mol for the adsorption of pyrazine into Al-CAU-13. This is quite reasonable since the activation energy for the adsorption of pyrazine is thus in the same range as the adsorption enthalpy for water in, for example, the Al-based MOF CAU-10.[53] Since water is actually exchanged for pyrazine during adsorption, this value seems very plausible. However, as mentioned above these interpretations should be considered tentative and it would be highly desirable to evaluate further breathing compounds during intercalation.

Conclusions

The adsorption of functionalised pyrazines into Al-CAU-13 indicates a rich structural diversity which originates mostly from the interplay of linker conformations and dominating host-guest interactions. In addition, we have demonstrated that the newly developed cell for in-situ PXRD measurements allows a sufficient temporal resolution for the measurement of adsorption processes at comparably low temperature. This opens the opportunity for the detailed analysis of diverse breathing processes which can be visualized by X-ray diffraction. The spatial resolution i.e. reflection overlap can be a substantial problem and this is where future improvements will start.

Acknowledgements

We are much obliged for the help of Uta Ruett (DESY Hamburg) during the in-situ measurements. The assistance of Milan Köppen and Dirk Lenzen (CAU Kiel) during the work presented in this manuscript is also gratefully acknowledged.

Notes and references

[1] N. Stock and S. Biswas, *Chem. Rev.*, 2012, **112**, 933.
[2] M. Eddaoudi, J. Kim, N. Rosi, D. Vodak, J. Wachter, M. O'Keeffe, O. M. Yaghi,, *Science*, 2002, **295**, 469.
[3] B. Van de Voorde, B. Bueken, J. Denayer and D. De Vos, *Chem. Soc. Rev.*, 2014, **43**, 5766.
[4] P. Valvekens, F. Vermoortele, D. De Vos, *Catal. Sci. Technol.*, 2013, **13**, 1435.
[5] J. Heine, K. Müller-Buschbaum, *Chem. Soc. Rev.*, 2013, **42**, 9232.
[6] J. Canivet, A. Fateeva, Y. Guo, B. Coasne, D. Farrusseng, *Chem. Soc. Rev.*, 2014, **43**, 5594.
[7] G. Ferey, *Z. Anorg. Allg. Chem.*, 2012, **638**, 1897.
[8] A. Schneeman, V. Bon, I. Schwedler, I. Senkovska, S. Kaskel and R.A. Fischer, *Chem. Soc. Rev.,* 2014, **43**, 6062.
[9] C. Serre, C. Mellot-Draznieks, S. Surble, N. Audebrand, Y. Filinchuk, G. Ferey, *Science*, 2007, **315**, 1828.
[10] G. Ferey, C. Serre, *Chem. Soc. Rev.*, 2009, **38**, 1380.
[11] J. P. S. Mowat, S. R. Miller, A. M. Z. Slawin, V. R. Seymour, S. E. Ashbrook, P. A. Wright, *Micropor. Mesopor. Mat.,* 2011, **142**, 322.
[12] C. Serre, F. Millange, C. Thouvenot, M. Noguès, G. Marsolier, D. Louër, G. Ferey, *J. Am. Chem. Soc.,* 2002, **124***,* 13519.
[13] T. R. Whitfield, X. Wang, L. Liu, A. J. Jacobson, *Solid Stat. Sci.*, 2005, **7**, 1096.
[14] T. Loiseau, C. Serre, C. Huguenard, G. Fink, F. Taulelle, M. Henry, T. Bataille, G. Ferey, *Chem.- Eur. J.*, 2004, **10**, 1373.
[15] C. Volkringer, T. Loiseau, N. Guillou, G. Ferey, E. Elkaim, A. Vimont, *Dalton Trans.,* 2009, 2241.
[16] V. Anokhina, M. Vougo-Zanda, X. Wang, A. J. Jacobson, *J. Am. Chem. Soc.,* **2005**, *127*, 15000.
[17] L. Wang, T. Song, C. Li, J. Xia, S. Wang, L. Wang, J. Xu, *J. Solid. State Chem.*, 2012, **190**, 208.
[18] I. H. Kim, X. Wang, A. J. Jacobson, *Solid State Sci.*, 2010, **12**, 76.
[19] F. Niekiel, M. Ackermann, P. Guerrier, A. Rothkirch, N. Stock, *Inorg. Chem.*, 2013, **52**, 8699.
[20] H. Reinsch, D. De Vos, *Micropor. Mesopor. Mater.*, 2014, **200**, 311.
[21] F. Niekiel, J. Lannoeye, H. Reinsch, A. S. Munn, A. Heerwig, I. Zizak, S. Kaskel, R. I. Walton, D. de Vos, P. Llewellyn, A. Lieb, G. Maurin, N. Stock, *Inorg. Chem.*, 2014, **53**, 4610
[22] B. Bueken, F. Vermoortele, D. E. P. Vanpoucke, H. Reinsch, C.-C. Tsou, P. Valvekens, T. De Baerdemaeker, R. Ameloot, C. E. A. Kirschhock, V. Van Speybroeck, J. M. Mayer, D. De Vos, *Angew. Chem. Int. Ed.*, 2015, **54**, 13912.
[23] B. Bueken, F. Vermoortele, M. J. Cliffe, M. T. Wharmby, D. Foucher, J. Wieme, L. Vanduyfhuys, C. Martineau, N. Stock, F. Taulelle, V. Van Speybroeck, A. L. Goodwin, D. De Vos, *Chem. Eur. J.*, 2016*,* **22***,* 3264*.*
[24] H. Reinsch, R. S. Pillai, R. Siegel, J. Senker, A. Lieb, G. Maurin, N. Stock, *Dalton Trans.*, 2016, **45**, 4179.
[25] N. Pienack, W. Bensch, *Angew. Chem. Int. Ed.*, 2011, **50**, 2014.
[26] M. Søndergaard, K. J. Dalgaard, E. D. Bøjesen, K. Wonsyld, S. Dahl, B. B. Iversen, *J. Mater. Chem. A*, 2015, **3**, 18667.
[27] J. Houlberg, E. D. Bøjesen, C. Tyrsted, A. Mamakhel, X. Wang, R. Su, F. Besenbacher, B. B. Iversen, *Cryst. Growth Des.*, 2015, **15**, 3628.
[28] E. Antonova, B. Seidlhofer, J. Wang, M. Hinz, W. Bensch, *Chem. Eur. J.*, 2012, **18**, 15316.
[29] R. Kiebach, N. Pienack, M.-E. Ordolff, F. Studt, W.Bensch, *Chem. Mater*. 2006, **18**, 1196.
[30] N. Pienack, C. Näther, W. Bensch, *Eur. J. Inorg. Chem.*, 2009, 937.
[31] R. J. Francis, S. O'Brien, A. M. Fogg, P. S. Halasyamani, D. O'Hare, T. Loiseau, G. Ferey, *J. Am. Chem. Soc.*, 1999, **121**, 1002.
[32] Y. Zhou, Q. Zhang, Y. Lin, E. Antonova, W. Bensch, G.R. Patzke, *Sci. China Chem.,* 2013, **56**, 435.
[33] Y. Zhou, E. Antonova, Y. Lin, J.-D. Grunwaldt, W. Bensch, G. R. Patzke, *Eur. J. Inorg. Chem.*, 2012, **5**, 35.
[34] B. Seidlhofer, N. Pienack, W. Bensch, *Z. Naturforsch.,* 2010, **65b**, 937.
[35] R. El Osta, M.Frigoli, J.Marrot, M.E. Medina, R.I. Walton, F. Millange, *Cryst. Growth Des.*, 2012, **12**, 1531.
[36] E. Stavitski, M. Goesten, J. Juan-Alcaniz, A. Martinez-Joaristi, P. Serra-Crespo, A. V. Petukhov, J. Gascon, F. Kapteijn, *Angew. Chem. Int. Ed.*, 2011, **50**, 9624.
[37] T. Ahnfeldt, J. Moellmer, V. Guillerm, R. Staudt, C. Serre, N. Stock, *Chem.-Eur. J.*, 2011, **17**, 6462.
[38] M. Feyand, C. Näther, A. Rothkirch, N. Stock, *Inorg. Chem.*, 2010, **49**, 11158.
[39] M. Feyand, M. Köppen, G. Friedrichs, N. Stock, *Chem. Eur. J.*, 2013, **19**, 12537.
[40] Y. Wu, M. I. Breeze, G. J. Clarkson, F. Millange, D. O'Hare, R. I. Walton, *Angew. Chem. Int. Ed.*, 2016, **55**, 4992.
[41] Topas Academics 4.2, Coelho Software, 2007.
[42] Materials Studio Version 5.0, Accelrys Inc., San Diego, CA, 2009.
[43] George A. Jeffrey, An Introduction to Hydrogen Bonding (Topics in Physical Chemistry), Oxford University Press, USA, 1997.
[44] M. Krüger, R. Siegel, A. Dreischarf, H. Reinsch, J. Senker, N. Stock, *Micropor. Mesopor. Mater.*, 2015, **216**, 27.
[45] H. Reinsch, M. Krüger, J. Wack, J. Senker, F. Salles, G. Maurin, N. Stock, *Micropor. Mesopor. Mater.*, 2012, **157**, 50.
[46] T. R. Whitfield, X. Wang, L. Liu, A. J. Jacobson, *Solid State Sci.*, 2005, **7**, 1096.
[47] M. Vougo-Zanda, J. Huang, E. Anokhina, X. Wang, A. J. Jacobson, *Inorg. Chem.*, 2008, **47**, 11535.
[48] F. Millange, N. Guillou, M. E. Medina, G. Ferey, A. Carlin-

Sinclair, K. M. Golden, R. I. Walton, *Chem. Mater.*, 2010, **22**, 4237.
[49] N. Heidenreich, *manuscript in preparation.*
[50] This might seem unnecessary to mention, however, usually reactions to be measured at synchrotron facilities need to be first started and afterwards the experimental hutch is locked. Thus most often a delay of 1-3 minutes exists between initiation of the reaction and the start of the measurements.
[51] J. D. Sharp, J. H. Hancock, *J. Am. Ceram. Soc.*, 1972, **55**, 74.
[52] M. Avrami, *J. Chem. Phys.*, 1939, **7**, 1103.
[53] D. Fröhlich, E. Pantatosaki, P. D. Kolokathis, K. Markey, H. Reinsch, M. Baumgartner, M. A. van der Veen, D. E. De Vos, N. Stock, G. K. Papadopoulos, S. Henninger, C. Janiak, *J. Mat. Chem. A*, 2016, **4**, 11859.